

# The air quality forecast of PM<sub>10</sub> in Beijing with Community Multi-scale Air Quality Modeling (CMAQ) system: emission and improvement

Q. Wu<sup>1</sup>, W. Xu<sup>2</sup>, A. Shi<sup>2</sup>, Y. Li<sup>2</sup>, X. Zhao<sup>3</sup>, Z. Wang<sup>4</sup>, J. Li<sup>2</sup>, and L. Wang<sup>1</sup>

<sup>1</sup>College of Global Change and Earth System Science, Beijing Normal University, Beijing 100875, China

<sup>2</sup>Beijing Municipal Environmental Protection Monitoring Center, Beijing 100048, China

<sup>3</sup>Environmental Meteorology Forecast Center of Beijing-Tianjin-Hebei, Beijing 100089, China

<sup>4</sup>State Key Laboratory of Atmospheric Boundary Layer Physics and Atmospheric Chemistry (LAPC), Institute of Atmospheric Physics, Chinese Academy of Sciences, Beijing 100029, China

Correspondence to: Q. Wu (wqizhong@bnu.edu.cn) and X. Zhao (xjzhao@ium.cn)

## Abstract

The MM5-SMOKE-CMAQ model system, which was developed by the United States Environmental Protection Agency (US EPA) as the Models-3 system, has been used for daily air quality forecasts in the Beijing Municipal Environmental Monitoring Center (Beijing MEMC), as a part of the Ensemble Air Quality Forecast System for Beijing (EMS-Beijing) since the Olympic Games 2008. According to the daily forecast results for the entire duration of 2010, the model shows good performance in the  $PM_{10}$  forecast on most days but clearly underestimates  $PM_{10}$  concentration during some air pollution episodes. A typical air pollution episode from 11–20 January 2010 was chosen, where the observed air pollution index of particulate matter ( $PM_{10}$ -API) reached to 180 while the forecast's  $PM_{10}$ -API was about 100.

In this study, three numerical methods are used for model improvement: first, enhance the inner domain with 3 km resolution grids: the coverage is expanded from only Beijing to the area including Beijing and its surrounding cities; second, add more regional point source emissions located at Baoding, Landfang and Tangshan, which is to the south and east of Beijing; third, update the area source emissions, which includes the regional area source emissions in Baoding and Tangshan and the local village–town level area source emissions in Beijing. The last two methods are combined as the emissions updated method. According to the model sensitivity testing results by the CMAQ model, the emissions updated method and expanding model domain method can both improve the model performance separately. But the expanding model domain method has better ability on capturing the peak values of  $PM_{10}$  than the emission updated method due to better produce the pollution transport process in this episode. As a result, the hindcast results (“New(CMAQ)”), which is driven by the updated emissions in the expanded model domain, shows a much better model performance in the national standard station-averaged  $PM_{10}$ -API. The daily hindcast  $PM_{10}$ -API reaches 180 and is much closer to the observed, and has a high correlation coefficient of 0.93. The correlation coefficient of the  $PM_{10}$ -API in all Beijing MEMC stations between the

hindcast and observation is 0.82, obviously higher than the forecast's 0.54. The FAC2 increases from 56 % in the forecast to 84 % in the hindcast, and the NMSE decreases from 0.886 to 0.196. The hindcast also has better model performance in  $PM_{10}$  hourly concentrations during the typical air pollution episode. The updated emissions accompanied with suitable domain in this study improved the model performance significantly in Beijing area.

## 1 Introduction

In recent ten years, the air quality problems have caused particular concern in most of China, especially after the extreme air pollution episode happened in multiple cities of North China in January 2013. In such a heavy air pollutant environment, the people is eager to have access to reasonable air quality predictions, to provide advance notice for future air pollution events with potential adverse health effects, and the government can take necessary short-term emissions reduction measures to improve the air quality, as they have done during the Beijing Olympic Games. Wu et al. (2010a) and Wang et al. (2010) reported that the  $PM_{10}$  related emission has reduced about 200 tons per day at that time. The air quality models are the effective tools to achieve air quality forecasts and also for the policy decisions, since they can provide scientific advice for air pollution control measures (Feng et al., 2007).

Actually, the Ensemble Air Quality Forecast System for Beijing (EMS-Beijing) was build and has been used for air quality forecast since the Olympic Games year 2008 (Wang et al., 2009; Wu, 2010). The ensemble system contains the Community Multiscale Air Quality (CMAQ) modeling system v4.4 (Byun and Ching, 1999; Byun and Schere, 2006), the three-dimensional Comprehensive Air Quality Model with extensions (CAMx) v4.0 (ENVIRON, 2002) and the Nested Air Quality Prediction Modeling System (NAQPMS) (Wang et al., 2006), using the unified meteorological field and emissions provided respectively by the fifth-generation Mesoscale Model (MM5) and the Sparse Matrix Operator Kernel Emissions (SMOKE) (Houyoux and Vukovich, 1999).

All the models adopt the same model domain with same grid size and resolution, and it is a good platform for air quality modeling study, to evaluate and improve the models.

The ensemble forecast system has had successful forecasts since the Olympic Games in 2008, and has been introduced in Shanghai, Guangzhou and other cities (Wu, 2010; Wu et al., 2010a, 2012) in the past few years. In this study, we collect the daily forecast results of the CMAQ model, which is a one member model in ESM-Beijing for the entire duration of 2010 for the model evaluation. The results show that the model shows a good performance in most days but underestimate obviously in some air pollution episodes. Thus, a typical air pollution episode from 11–20 January 2010 was chosen for the model evaluation and improvement, in which the air pollution index (API) of particulate matter ( $PM_{10}$ ) observed by Beijing MEMC reaches 180 while the CMAQ prediction of  $PM_{10}$ -API is about 100. Some numerical methods are used for the model improvement for the hindcast simulation in this study, the methods including model setup and emission updated.

The remainder of the paper is organized as follows. Section 2 would give the model description and setup in the forecast system, including meteorological field and air quality model descriptions in Sects. 2.1 and 2.2, model domain in Sect. 2.3, and the emission inventory and processes with SMOKE model in Sect. 2.4, including area, point and mobile source emissions. The Sect. 3 gives the model performance and improvement of the CMAQ model system, the observation data is described in Sect. 3.1, and the forecast system is shown in Sect. 3.2. The improvement methods are presented in Sect. 3.3, one is to enhance in the inner domain, the other is to update the anthropogenic emissions, including area and point source emissions; more details and model evaluation of the improvement would be discussed in the Sect. 3.3, and the model evaluation and discussion about  $PM_{10}$  in the model sensitivity testings when the model domain expanded, the emissions updated, and the hindcast simulation (included the all improvement methods) is in Sect. 3.4. The conclusions are present in Sect. 4.

## 2 Model description of the forecast system

The MM5-SMOKE-CMAQ model system, as one model member of of the ensemble air quality forecast system in Beijing (EMS-Beijing), has been used for daily air quality forecast since 2008. The framework of the model system is shown in Fig. 1: the MM5 model is used to generate the meteorological field, the SMOKE model is applied to deal with the emissions inventory and provides 3-D gridded emission data for the air quality model, and the CMAQ model provides the concentration of the gas- and particle-species for daily air quality forecast.

### 2.1 Meteorological field

In the model system, the Fifth-generation NCAR/Penn State Mesoscale Model (MM5) v3.6 (Grell et al., 1994) is used to generate the meteorological field for the SMOKE and CMAQ model. The selected schemes for the present study include the simple ice for explicit moisture scheme, Grell cumulus scheme, MRF for PBL scheme and cloud scheme for atmospheric radiation according to the study of Gao et al. (2007) and Wu et al. (2010b).

As shown in the “meteorology” part of Fig. 1, there are five modules to be used, including TERRAIN, pregrid, regridder, INTERPF, and MM5 modules. Both the “pregrid” and “regridder” modules are a part of REGRID, which would create the first-guess meteorological field on MM5 grids, the “pregrid” could read the GRIB1-formatted global dataset and prepare them as MM5 formatted. In the forecast system, the National Centers for Environmental Prediction (NCEP) Global Forecast System (GFS) data set, which was taken from the FTP site: <ftp.ncep.noaa.gov>, with  $0.5^\circ \times 0.5^\circ$  spatial resolution, is used as the initial and boundary conditions for the regional meteorological model MM5, and the daily data sets of the 00, 24, 48, 72, 96 h forecast at 20:00 local time on the last day have been downloaded from the websites with the wget tool and cron service in Linux system. Once the downloading is finished, the cnvgrib tool, which is built from <http://www.nco.ncep.noaa.gov/pmb/codes/GRIB2/> to achieve data

format conversion between GRIB1 and GRIB2 formatted, is used to convert the GRIB2-formatted GFS data sets to GRIB1-formatted before the “pregrid” module. And then, the MM5 modules begin running to prepare the meteorological field for the emission and air quality model.

5 In the forecast system, we design csh scripts to schedule the process of the modules, whose scripting feature is to check if the downloading or the running of the previous module is finished.

## 2.2 Air quality model descriptions

The CMAQ model is used for regional and urban-scale air quality simulation of tropo-  
10 spheric ozone, acid deposition, visibility, and particulate matter (Byun and Ching, 1999; Byun and Schere, 2006) and has been widely used over the world including East Asia (An et al., 2007; Zhang et al., 2006). It contains state-of-science parameterizations of atmospheric processes affecting transport, transformation, and wet/dry deposition. There are five modules of the CMAQ version 4.4 used in the forecast system as shown  
15 in the “CMAQ” part of Fig. 1. The CMAQ Chemistry-Transport Model (CCTM) is the main module, and the CB-VI scheme for the gas-phase chemistry (Gery et al., 1989), MEBI scheme for the gas-phase chemical solver, RADM scheme for the aqueous-phase chemistry and AERO3 module for aerosol calculation (Binkowski and Roselle, 2003) are applied in the forecast system. The Meteorology Chemistry Interface Processor (MCIP) links MM5 model results with CCTM module to provide a complete set  
20 of the meteorological data needed for the air quality simulations (Appel et al., 2010). The photolysis rate model (JPROC) is used to calculate the a day specific clear sky photolysis rate look-up table for latitudinal and elevation bands for each photochemical reaction in the gas-phase chemistry scheme base on work published by Demerjian et al. (1980) (Cruickshank, 2008).  
25

The initial conditions (ICON) and boundary conditions (BCON) are based on clean-troposphere vertical profile concentration fields for the beginning of the first day simulation and the grids surrounding the outer domain “D1”. The initial conditions of the fol-

lowing day simulation are based on the 24 h prediction in the forecast results of the day before. The boundary conditions of the inner domains are retrieved from their mother domain because the CMAQ model used a one-way nesting scheme in the forecast system, and its domain setup will be described in Sect. 2.3.

5 In this study, we collect the air pollution index (API) as the observation for the model evaluation, which is published on the website of the Beijing Environmental Protection Bureau (Beijing EPB), but only the primary air pollutant in each station. Particulate material is the primary air pollutant in most cities in North China, such as Beijing, that the PM<sub>10</sub> has the most observation samples for the model evaluation.  
10 The PM<sub>10</sub> comes from a great variety of emissions sources, including fugitive dust, power plants, cement and pottery manufacturing, etc., while some are produced by oxidization of gaseous pollutant or photochemical reactions as second aerosol, thus, several species must be included in PM<sub>10</sub> numerical simulation. According to Byun and Ching (1999) and Binkowski and Roselle (2003), the accumulation and Aitken mode of sulfate mass (ASO<sub>4</sub>), ammonium mass (ANH<sub>4</sub>), nitrate mass (ANO<sub>3</sub>), anthropogenic secondary/primary/biogenic organic mass (AORGA/AORGPA/AORGB), elemental carbon mass (AEC), unspecified anthropogenic mass (A25) and coarse mode marine/soil-derived/unspecified anthropogenic mass (ACORS/ASEAS/ASOIL) are included in PM<sub>10</sub> numerical simulation of the CMAQ model:

$$20 \quad \text{PM}_{10} = \text{ASO}_4 + \text{ANH}_4 + \text{ANO}_3 + \text{AORGA} + \text{AORGPA} + \text{AORGB} + \text{AEC} + \text{A25} \\ + \text{ACORS} + \text{ASEAS} + \text{ASOIL}. \quad (1)$$

The translation of the concentration to the API is shown in Appendix A. In this study, we translate PM<sub>10</sub> concentration to PM<sub>10</sub>-API in the CMAQ model result, to compare with the observed PM<sub>10</sub>-API in Beijing MEMC stations.

## 2.3 Model domain

Four nested grids of the horizontal spatial resolution in 81 km, 27 km, 9 km and 3 km are used for both MM5 and CMAQ models in the forecast system, and the inner two domains (D3 and D4) are shown in the left of Fig. 2.

5 The center of the model domain is located at (35.0° N, 110° E) and its two true latitude lines are (30° N, 60° N). The outermost domain (D1) has a  $83 \times 65$  grid to cover East Asia, while the second domain (D2) has a  $61 \times 58$  grid to include North China, which covers the surrounding provinces of the Beijing Municipality, and the power plant emissions in those provinces are collected from Chinese Research Academy of Environmental Sciences (CRAES) as one part of the local emission inventories. The third  
10 domain (D3) has  $79 \times 70$  grids of 9 km resolution and consists of Beijing, Tianjin, most area of Heibei province and one part of other surrounding provinces in North China. In Hebei province, other than the local power plant emission inventory, the local inventories about other industrial emissions are collected from Beijing University of Technol-  
15 ogy (BUT), and handled as the point sources. In the forecast system, the fourth domain (D4) has a  $73 \times 64$  grid and only covers Beijing Municipality, where more detailed local emissions inventories are included and will be presented in Sect. 2.4.

Moreover, there are 23 sigma vertical layers unequally distributed in the MM5 model with the top layers at 10 hPa and 6 layers below 1 km; the CMAQ model has 14 vertical  
20 layers where the lower 10 layers are same as the MM5 model. The height of the surface (lowest) layer at approximately 35 m.

## 2.4 Emission inventory and processes

The Sparse Matrix Operator Kernel Emissions (SMOKE) v2.1 (Houyoux and Vukovich, 1999) model is applied to improve the emissions process and provides model-ready  
25 emissions for the air quality model. We consider the emissions as the area, point and mobile sources in the model system as shown in Fig. 1.



Three emission inventories are used in this study: (1) the regional emissions in East Asia from Transport and Chemical Evolution over the Pacific (TRACE-P) project (Streets et al., 2003; Streets et al., 2006) without the power plant emissions, (2) the Intercontinental Chemical Transport Experiment-Phase B (INTEX-B) power plant emissions inventory with 30 min spatial resolution (Zhang et al., 2009), and (3) the local emission inventories covering the North China region, especially in Beijing; emissions inventories were used in Wu et al. (2010c, 2011). The 6 min spatial resolution TRACE-P emissions are handled as area sources while the large point sources (Ips sector in TRACE-P emission) are treated as point sources. The INTEX-B power plant emissions are taken as point source emissions and replace the power plant emissions in TRACE-P emissions, and the local emission inventories are taken as area, point and mobile source emissions with the detail process followed.

#### **2.4.1 Area source emissions**

The area source emissions are taken with a “top-down” approach, given a total emission and assigned to a model grid boxes with relative spatial distribution factor, such as population, road density, etc. As shown in the Fig. 3, the area emissions were spatially allocated according to the Land Scan 2005 Global Population Database (Dobson et al., 2000) and other spatial distribution factor; the emissions temporal variation is assigned from a “profile” file, while the species allocation is based on SPECIATE 4.0 species database (Mobley et al., 2007).

Usually, the statistics emission inventories in China are at the county level, or city level, or even provincial level, statistics in the administrative boundaries. Thus, in order to facilitate updating the local emission inventories, we transform all regional area source emission inventories into county-level inventories. In the forecast system, the TRACE-P industry (ind), transportation (tra), domestic biofuel (dob), domestic fossil fuel (dof) emissions, livestock ammonium emissions and biogenic emissions (Streets et al., 2003) have been converted from latitude–longitude gridded to county-level emission inventories using the geographical statistics tool in ArcGIS platform.

The local area source emissions inventories in Beijing include residential fossil fuel (dof), residential biofuel (dob), unorganized industrial area source, building operations and mutation fugitive dust emission, road fugitive dust emission and anthropogenic ammonia emission; they are county-level inventories in the forecast system. In the SMOKE model system, the residential fossil fuel (dof) and residential biofuel (dob) emissions are used to replace the domestic fossil fuel (dof) and domestic biofuel of the TRACE-P emission in Beijing counties, and the other categories emissions are added directly. In order to obtain high-resolution emissions, the residential area source emissions in Beijing have been allocated based on the Land Scan population data, and the spatial distribution of the population in Beijing Municipality is shown in the right part of Fig. 3. Besides, the road fugitive dust emission essentially from road surface is spatially distributed according to traffic density in Beijing, with the compiled road statistics including arterial and local ways.

The spatial distribution of area source emissions in the inner domain (D4) of the forecast system is presented on the Fig. 3, we can see that the high-PM<sub>10</sub> emissions correspond to high-population density, with the highest emission being located in urban Beijing.

#### **2.4.2 Point source emissions**

Point source emissions processing in SMOKE model focuses on converting annual, daily, or hourly emissions to hourly, gridded model-ready emissions used by air quality model (UNC, 2010). Same as the area source emissions, the temporal variation and species allocation of point source emissions are given by a “profile” file.

The spatial allocation of point source emissions in SMOKE is very straightforward in that it simply determines which cell the point source’s longitude–latitude coordinates are in and assigns them to model grid cells. Based on the Briggs algorithm (Briggs, 1972, 1984), the SMOKE model uses the stack and meteorological parameters to compute the plumes’ distributions into the vertical layers that the plumes intersect, and put the emission into the vertical layers. The stack parameters, including the stack height,

diameter and exit gas temperature, could be collected from the point source emission inventory; the meteorological parameters are retrieved from the MM5 model results with the MCIP module (Houyoux et al., 1999).

As mentioned above, the point source emissions used in the forecast system includes the TRACE-P large point source (lps), 0.5° INTEX-B power plant emissions and the local point source emissions. The power plant emissions of the local database covers Beijing and its surrounding provinces including Tianjin, Hebei, Shanxi, Inner Mongolia and Shandong provinces, with the based year 2006. The local emission inventories have more specific information about the position, and are used to replace the INTEX-B power plant emissions in those provinces. But from 2006 to 2008, some cleaner combustion and flue gas treatment in power plant have been taken step by step, including dust control improvement, closure of high-pollution small units, adding desulfurization patenting agent and low-NO<sub>x</sub> combustion. Thus, the power plant emissions in Beijing have been updated according to Hao et al. (2008) and the National Notice “The coal-fuel units Flue Gas Desulfurization construction Notice” with the website at [http://www.sepa.gov.cn/info/gw/gg/200703/t20070308\\_101419.htm](http://www.sepa.gov.cn/info/gw/gg/200703/t20070308_101419.htm).

In Hebei province, there are 418 point source emissions collected and introduced into the point source inventory of the SMOKE model, including the main industrial emissions in Hebei provinces from Beijing University of Technology (BUT), which is used by Wu et al. (2011). In Tianjin and Beijing Municipality, there are more detailed point source emissions with full stack parameters, which are provided by CRAES and Beijing Municipal Environmental Protection Bureau (Beijing EPB), and used to update the heating boiler, steel, cement and other industrial emissions in Tianjin and Beijing. In that emission inventory, there are 493 higher point source emissions, whose stack height is above 45 m, 1970 lower point source emissions in Tianjin, and 652 point source emissions in Beijing. Those local point source emissions are used to replace the related category emissions in the SMOKE model.

### 2.4.3 Mobile source emission

Based on the road network and the traffic flow from Beijing Transport Research Center (BTRC, 2007), Wu et al. (2010c) estimated the spatial distribution of the mobile source emissions using the SMOKE mobile module, and used it to assess the impact of vehicle traffic restriction on air quality in Beijing from 17 to 20 August 2007.

The on-road mobile source emissions without vehicle traffic restriction in that study (Wu et al., 2010c) have been used in the EMS-Beijing forecast system, the criteria emission factors using MOBILE6 is computed with the forecast meteorology data (UNC, 2010), and its meteorological field is provided from the everyday MM5 model results through MCIP module. The mobile source emissions provide 90 % CO, 50 % NO<sub>x</sub> and 45 % VOCs emissions, but a small percentage of SO<sub>2</sub>, PM<sub>10</sub> and PM<sub>2.5</sub> emissions in Beijing in the forecast system.

### 2.4.4 The total emission

The total emissions used in the forecast system are calculated from the daily report of the SMOKE model output, and shown in Table 1 with other published inventories. Compared those emission inventories, we found that there is much uncertainty in the emission inventory. For example, in Beijing the CO emission range is from 1021.8 kt yr<sup>-1</sup> in An et al. (2007) to 2591.0 kt yr<sup>-1</sup> in Zhang et al. (2009), and the PM<sub>10</sub> emission is about 66.0 in Streets et al. (2007) to 168.0 kt yr<sup>-1</sup> in Zhao et al. (2012). The PM<sub>2.5</sub> emission has the biggest uncertainty, where only 27.2 kt yr<sup>-1</sup> estimated by Streets et al. (2007), and 162.0 kt yr<sup>-1</sup> in Cao et al. (2011). The uncertainty comes from the investigation about emissions, the base year of the investigation, the emission factor of each sector, the active rates (e.g. energy consumption or industrial production) and others.

The forecast system has the lowest NO<sub>x</sub> and VOCs emissions in Beijing compared with those studies. The NO<sub>x</sub> and VOCs emissions, which the mobile source emissions contributed nearly a half, may be underestimated in the forecast system. The mobile source emissions in Beijing has been estimated based on the investigation of road

networks and traffic flow in 2006 that would underestimate the vehicle numbers and traffic flow, therefore, underestimate the CO, NO<sub>x</sub> and VOCs emissions.

The forecast system also has the lowest emissions of SO<sub>2</sub> in Beijing because it includes “Flue Gas Desulfurization” to decrease SO<sub>2</sub> emissions in the inventory. In the annual report “State of the Environment Bulletin” published by Beijing EPB, the SO<sub>2</sub> emission in the year 2010 was 104.4 tons (Beijing EPB, 2011). Thus, the SO<sub>2</sub> emission in the forecast system for the year 2010 in Beijing is reasonable but may be underestimated.

### 3 Model performance and improvement

In this study, we collect the observation and forecast results in the entire duration of 2010 for the model evaluation and improvement. One typical air pollution episode, in which the forecast can not give the expected peak, is chosen and studied in this section.

#### 3.1 Observation data for model evaluation

There are 27 stations in Beijing Municipal Environmental Monitoring Center (Beijing MEMC) air quality monitoring network in the year 2010 with the location shown as “black mark” in Fig. 5. Twelve of them are the National Standard Air Quality Observation Stations (NSAQ Stations) which are marked as “squares” in Fig. 5, eight stations in the urban Beijing, three stations in the county town, and the Dingling station is the regional background NSAQ station. Except Dingling, the other eleven stations located at urban area, which includes cities, towns or conurbations. The air pollution index (API) value is daily reported and published at the website <http://www.bjepb.gov.cn/bjepb/341240/index.html>, the averaged PM<sub>10</sub>-API in the NSAQ stations have been collected as the observation for the model evaluation, and daily reported API of the main pollutant in

all 27 stations have been also collected as the observation and compared with CMAQ model outputs.

Besides that, the  $PM_{10}$  hourly concentration averaged in NSAQ stations have been provided by Beijing MEMC and used for the model evaluation about the model ability to reproduce the hourly concentration. And the  $PM_{10}$  hourly concentration in Beijing's surrounding areas are also collected to evaluate the model performance in the surrounding areas and be presented in the supplement material. The manuscript focuses on the model performance in Beijing.

### 3.2 Model performance in the forecast

In this study, the daily forecast results of the CMAQ model in the entire duration of 2010 are collected for the model evaluation. The scatter diagram of the averaged  $PM_{10}$ -API in the NSAQ Stations and forecasted are shown in Fig. 6. As shown in the figure, most observed-forecasted points are close to the model perfect line " $y = x$ ", which indicates that the model on the forecast shows a good performance in most days. However, all of the observed-forecasted points are below the line " $y = 150$ " through some points can reach to the line " $x = 250$ ". This illustrates that the forecasted  $PM_{10}$ -API is lower than 150 but the observation can reach to 250. The forecast results are underestimated when the  $PM_{10}$ -API value is high, in which a serious air pollution episode occurred.

As mentioned above, the model in the forecast shows a good model performance on most days but clearly underestimates in some air pollution episodes. In order to improve the model performance, a typical air pollution episode from 11–21 January 2010 was chosen, in which the averaged air pollution index of particulate matter ( $PM_{10}$ -API) in NSAQ stations in Beijing reaches to 180, while the CMAQ prediction is about 100 as shown in Fig. 7. The green solid line in Fig. 7 presents the averaged  $PM_{10}$ -API prediction in the ten NSAQ stations in Beijing, which is predicted by CMAQ model in the forecast system, and compared with the observed "red solid line" to show its model performance. It can be found that the CMAQ model underestimates the peak value during the air pollution episode on 19 January.

Besides the averaged  $PM_{10}$ -API in NSAQ stations, the main pollutant API in all 27 stations, not only NSAQ stations but also non-NSAQ stations as “triangle” marked in Fig. 5, also be collected to verify the modeled  $PM_{10}$ . The main pollutant in all 27 stations during the typical episode was almost  $PM_{10}$ . There have been 270 API samples collected, 199 of those samples are marked as “ $PM_{10}$ , which is the main pollutant”, 6 samples are  $SO_2$ , and other samples are “degree I” that are not marked as the main pollutant. Thus, more than 97 % of the main pollutant in Beijing is  $PM_{10}$ . Actually, the main pollutant in “degree I” samples are  $PM_{10}$ , and are confirmed by Beijing MEMC. The missing  $PM_{10}$  samples in these 27 stations are also completed by Beijing MEMC.

Compared with the observation, the maximum of the  $PM_{10}$ -API in all stations predicted by the CMAQ model in the forecast did not exceed 150 during the air pollution episode, but the maximum of the observed has reached to 300, as shown in the “red” scatter diagram of Fig. 8.

### 3.3 Model improvement

In this study, three numerical methods are used for the improvement in air quality forecast in Beijing.

First, we enlarge the inner domain, the D4 domain with 3 km resolution grids, from which domain the forecast results are obtained. The original domain in the forecast system only covers Beijing Municipality, with  $73 \times 64$  grids of 3 km resolution. In the new simulation, the western boundary of the domain moves westward to the western boundary of Hebei province, the northern to the northern boundary of Hebei province, the eastern to the eastern boundary of Hebei province, and the southern to the Tianjin Municipality. As shown in Fig. 2, the new D4 domain has  $160 \times 124$  grids, and covers Beijing and its surrounding cities, including Zhangjiakou, Chengde, Tangshan, Langfang, Baoding and Tianjin Municipality.

Second, we add more point source emissions into SMOKE model, especially in the surrounding cities on the south and east of Beijing, to improve the model performance. In the south, there are 1935 point sources in Baoding that have been added into the

point source emissions inventory of SMOKE model. Baoding plays an important role on the  $PM_{10}$  contribution in the urban area of Beijing and its south counties (Wu et al., 2011). Landfang is another municipality that contributes quite a lot  $PM_{10}$  concentration to Beijing, it is on the southeast of Beijing and shows predominate role on the surrounding contribution to Beijing's eastern counties (Wu et al., 2011). Therefore, the point source emissions in Landfang are also collected to improve the simulation, and there are 609 point source emissions that have been added. Tangshan is to the east of Beijing, and it is the biggest emissions municipality in Hebei for  $SO_2$ ,  $NO_x$  and particle matter emissions (CCCPSC, 2011), and there are 1861 point source emissions in Tangshan that have been added. Those additional 4405 point source emissions include industrial, commercial and other catalogs. And their locations have been checked with Google Earth and other tools, which would be more accurate in the emission intensity and location in Baoding, Landfang and Tanshan. The new distribution of the point source emissions in the "new" D4 domain is shown in the right of Fig. 4.

Third, the area emissions updated. The area emissions in Baoding and Tangshan have been increased according to the emissions report in CCCPSC (2011), which are the two key cities for air pollutants and the total emissions of Baoding and Tangshan are shown in that emissions report. In order to get more accurate emissions, the Beijing stationary area emission inventory is updated from statistical county level to village–town level, which would provide a more detail spatial information for area emissions in Beijing. There are 18 counties in the forecast system, and more than 100 village–towns in the new simulation that the statistical unit of area emissions have great refinement, and will bring more accuracy in the distribution of the emissions.

### 3.4 Model performance in the new simulation

The improvement methods mentioned above includes two aspects: one is enhanced in the inner domain, the other is updated the emissions, including area and point source emissions. The model sensitivity testings by the CMAQ model with the new expanded domain and updated emissions in Sect. 3.3 is conducted from 10 to 21 January 2010,



and compared with the forecast results. The model performance of the  $PM_{10}$  in the model sensitivity testings are presented in this section.

### 3.4.1 Model performance of the daily $PM_{10}$ -API in the NSAQ stations

Fig. 7 showed the comparison of measured and modeled daily averaged  $PM_{10}$ -API in the NSAQ stations in Beijing urban area. The red and green solid line represents the observation and the forecast results in the forecast system. The model results driven by the updated emission without expanding the model domain was abbreviated as “NewEmis+FDomain(CMAQ)” and showed with the blue dashed line, the emissions updated includes the point and area source emissions updated. The modeled results driven by the forecast emission in the expanded model domain was abbreviated as “FEmis+NewDomian(CMAQ)” and presented with the green dashed line. The blue solid line is the final model results with all improvement methods and named as “New(CMAQ)” in Fig. 7. All the abbreviations were used with same meaning in the following text.

Compared the “Forecast(CMAQ)” and “FEmis+NewDomain(CMAQ)” results in Fig. 7, the averaged  $PM_{10}$ -API of the “FEmis+NewDomain(CMAQ)” results can reach to 140, while the peak value of the  $PM_{10}$ -API in the forecast was about 100. The mean bias of the “FEmis+NewDomain(CMAQ)” is  $-15.4$ , better than the forecast’s  $-24.7$ . The normalized mean square error (NMSE) of the “FEmis+NewDomain(CMAQ)” is 0.082, also much better than the forecast’s 0.251 as shown in Table. 2. And the correlation coefficient increases from 0.895 to 0.943 when the model domain was expanded with the forecast emissions in the CMAQ model. Furthermore, the air pollutant peak value of the “FEmis+NewDomain(CMAQ)” results occurs on 19 January, which is in agreement with the observation, while the forecast’s peak appears on 18 January and just a little change from 17 to 20 January. This indicates that the model domain expanded can improve the simulation performance in capturing the air pollution peak. Thus, the domain expanding can improve the model performance obviously, even the emissions have not been updated.

Compared the forecast results and the model results when the emissions have been updated in the original forecast model domain, as shown the “Forecast(CMAQ)” and “NewEmis+FDomain(CMAQ)” line in Fig. 7, the “NewEmis+FDomain(CMAQ)” is similar to the “Forecast(CMAQ)”. The peak of the PM<sub>10</sub>-API in the “NewEmis+FDomain(CMAQ)” is about 105, and the mean bias is -24.3, a little better than the forecast results. The NMSE between the “NewEmis+FDomain(CMAQ)” and the observation is 0.212, also slightly better than the forecast’s 0.251 as shown in Table. 2. This indicates that the method of “NewEmis+FDomain” showed slight improvement in simulating the temporal variation of PM<sub>10</sub> in Beijing area.

However, in the “New” expanded model domain, the same emission updated can improve the model performance obviously. As the “FEmis+NewDomain(CMAQ)” and “New(CMAQ)” shown in Fig. 7, they are simulated in the same expanded model domain but are driven by the forecast emissions and the updated emissions, respectively. The peak of the “New(CMAQ)” reaches to 180, much closer to the observed “red solid” line than the “FEmis+NewDomain(CMAQ)”, which peak is about 140. And the mean bias of the “New(CMAQ)” is -0.2, much better than the “FEmis+NewDomain(CMAQ)”; the NMSE of the “New(CMAQ)” is 0.042, also better than 0.082 of the “FEmis+NewDomain(CMAQ)”. The correlation coefficient of “New(CMAQ)” nears to the “FEmis+NewDomain(CMAQ)” at 0.931 shown in Table. 2. It illustrates that the same updated emission can improve the CMAQ model performance obviously than the original forecast emissions in the expanded model domain.

With the two group comparisons of the emission updated, we can found that the effect of emission updated will be obvious in the suitable model domain, such as the expanded model domain in this manuscript. This may be attributed to that more transport of pollutants in the surrounding areas are included in the expand domain. More transports in the surrounding areas are included in the expanded domain, because the CMAQ v4.4 model uses the one-way nesting, that several variables should be chosen as the boundary condition for the inner model domain and would underestimate

something through the boundary of the inner domain. The model sensitivity testings of another air quality model CAMx, which uses two-ways nesting, are presented in the supplement materials. The CAMx model has played much better model performance when the emissions has been updated without the model domain expanding, that the two-ways nested technology can help to produce the pollution transport process in this episode in the inner domain.

In the final model results with all improvement methods, the air pollutant peak value of the NSAQ station-averaged  $PM_{10}$ -API reaches to 180 on 19 January, and much closer to the observed “183” than the forecast’s “96”. The mean bias of the “New(CMAQ)” to the observation is  $-0.2$ , much better than  $-24.7$  in the forecast system, and the normal mean error (NME) is 15.9%, also better than 29.7% in the forecast. The correlation coefficient of the averaged  $PM_{10}$ -API in NSAQ stations is 0.93, and higher than 0.89 between the forecast and the observed. More significantly, the air pollutant peak value appears on 19 January, which is in agreement with the observation, and illustrates that the these methods would improve the occurrence of the air pollutant peak simulated in the model.

### **3.4.2 Model performance of the daily $PM_{10}$ -API in the all stations**

We also collect the  $PM_{10}$ -API in all Beijing MEMC stations during the air pollution episode as mentioned in Sect. 3.2 and the station map shown in Fig. 5 that covers all the Beijing counties.

The scatter diagram of the observed and simulated  $PM_{10}$ -API in all stations in the the model sensitivity testings are shown in Fig. 8, different colors stand for different model sensitivity testing results, and the statistical measures are presented in Table. 3. The fraction of predictions within a factor of two of the observations (FAC2) and the normalized mean square error (NMSE) are selected to evaluate the model performance in this section. The FAC2 is the most robust measure, which is not overly influenced by outliers(Chang and Hanna, 2004).

According to Fig. 8 and Table. 3, both the model domain expanded and the emission updated can improve the model performance: the MB and NMSE decreases obviously, the FAC2 reaches to 70% and 68%, and the correlation coefficient reaches to 0.78 and 0.72, respectively. The “New(CMAQ)” results, which is driven by the updated emission in the expanded model domain, includes the two aspects, play the best performance.

As shown in the figure, the blue “New(CMAQ)” points have the highest simulated value, which peak of the PM<sub>10</sub>-API reach to 220, and the “New(CMAQ)” points are closer to the model perfect line “ $y = x$ ” than the forecast’s points. After the improvement, the mean bias of the “New(CMAQ)” is  $-15.7$ , much better than the forecast’s  $-43.2$  in the PM<sub>10</sub>-API simulation; the correlation coefficient of the PM<sub>10</sub>-API in all stations between the “New(CMAQ)” and the observation is 0.82, obviously higher than 0.54 between the forecast and the observed. And the FAC2 of the PM<sub>10</sub>-API increases from 56% in the forecast to 84% in the final model results, which illustrates that there are more simulated samples that satisfy the FAC2 condition in the “New(CMAQ)” simulation. Furthermore, the NMSE of the PM<sub>10</sub>-API is 0.196, which is also much better than the forecast’s 0.886.

Based on the scatter plot (Fig. 8) and those statistical parameters, MB, R, FAC2 and NMSE between the simulation and observation, we can see that the CMAQ model gets much better model performance on the PM<sub>10</sub>-API simulation in all Beijing MEMC stations in the “New(CMAQ)” than in the forecast due to the improvement of the model domain and emissions discussed in Sect. 3.3.

### 3.4.3 Model performance of PM<sub>10</sub> hourly concentration

The observations of the PM<sub>10</sub> hourly concentration averaged in NSAQ stations have also been provided by Beijing MEMC, and used to evaluation the model ability on the simulation of the hourly concentration.

As shown in Fig. 9, the forecast and model sensitivity testings show good model performance for hourly concentrations during the first and smaller air pollution episode process from 11 to 15 January, and records the occurrence of the smaller episode on

14 January. In the second and “bigger” air pollution episode process, the observed  $PM_{10}$  concentration increases from  $50 \mu\text{g m}^{-3}$  to  $350 \mu\text{g m}^{-3}$  during 15–19 January, all the model sensitivity testings catch the first half accumulation process that the  $PM_{10}$  hourly concentration increases from  $50 \mu\text{g m}^{-3}$  to  $250 \mu\text{g m}^{-3}$  from 15 to 16, and also shows good performance in the process when the hourly concentration rapidly decreases to “ $50 \mu\text{g m}^{-3}$  and lower” only in several hours in the air pollutant dissipation process on 19 January.

But the forecast and “NewEmis+FDomain(CMAQ)” has no increases in the second half episode, where the observed hourly concentration increases from  $250 \mu\text{g m}^{-3}$  to  $350 \mu\text{g m}^{-3}$ , and the “FEmis+NewDomain(CMAQ)” and “New(CMAQ)” shows better performance in the second half episode in  $PM_{10}$  simulation, and the hourly concentration reaches to  $350 \mu\text{g m}^{-3}$ , which is the highest concentration in the observed hourly concentration during the air pollution episode. At the end, the “New(CMAQ)” gets the best model performance, and the model sensitivity testings with the expanded domain gets a better model performance, no matter the original forecast emissions.

The performance of the “FEmis+NewDomian(CMAQ)” is better than “NewEmis+FDomain(CMAQ)” may be attributed to the regional transport of the pollutants is better reproduced with expanding model domain. This pollution episode has been reported by Zhao et al. (2013), in which the pollutants in Beijing area are significantly increased by regional transport from south areas to Beijing. In forecast system, the pollutants outside of the inner domain(D4) that covered Beijing can only be transfer as a boundary condition to D4, and just part of pollutants can be selected into boundary conditions. With the model domain expended, all the pollutants in surrounding area can directly transport to Beijing and enhanced the modeling results than only increased emission without expanding domain.

Some statistical parameters of the  $PM_{10}$  hourly concentration in the forecast and “New(CMAQ)” is also presented in this study. The correlation coefficient between the simulation and observation increases from 0.77 in the forecast to 0.88 in the “New(CMAQ)”, which indicates that the “New(CMAQ)” has better tendency in hourly

concentration. The FAC2 of the hourly concentration increases from 62 % in the forecast to 74 % in the “New(CMAQ)”, and the NMSE decreases from 0.565 to 0.190, both illustrate that the “New(CMAQ)” has better model performance than the forecast in the  $PM_{10}$  hourly concentration.

5 The forecast shows bad model performance in high concentration in the simulation, where its simulated hourly concentration is lower than  $300 \mu\text{g m}^{-3}$  in this air pollution episode, and the daily  $PM_{10}$ -API is lower than 150 during the entire duration of 2010, where the API is translated from the daily concentration. The improvement fixes this issue partly in that the  $PM_{10}$  hourly concentration in the “New(CMAQ)” can reach  $350 \mu\text{g m}^{-3}$ , and the daily  $PM_{10}$ -API is able to reach 180, both are closer to the observation.

## 4 Conclusions

The MM5-SMOKE-CMAQ model system has been used in EMS-Beijing for daily air quality forecast in the past years. In this study, we introduce the model setup, meteorological field and emissions, including the emission inventory and processes in the forecast system. According to the model evaluation of  $PM_{10}$ -API for the entire duration of 2010, we found that the model shows a good model performance on most days but clearly underestimates some air pollution episodes. A typical air pollution episode was chosen to test the model improvement, including the model setup, emissions, etc.

20 In final, three numerical methods are adapted to the model improvement and presented in the this study. First, we enhance the inner “D4” domain, from  $73 \times 64$  to  $160 \times 124$  grids with 3 km resolution grids, to cover Beijing and its surrounding cities. Second, we add more regional point source emissions, where 4405 point source emissions, located at Baoding, Landfang and Tangshan, have been added into the point source emission inventory in SMOKE model. Third, we increase regional area source emissions in Baoding and Tangshan according to CCCPSC (2011), and update Beijing

area source emissions from statistical county level to village–town level to increase the resolution of the area inventory.

Compared the model evaluation about particle matter in different model sensitivity testings during the typical air pollution episode, we have found that the hindcast(“New(CMAQ)”), includes the domain expanded and emissions updated, shows a much better model performance. One obvious evidence that the hindcast’s averaged  $PM_{10}$ -API in NSAQ stations can reach to 180, and much closer to the observed “183”, while its hourly concentration can reach to the “observed”  $350 \mu\text{g m}^{-3}$ , but the forecast can not reach. In the simulation of the averaged  $PM_{10}$ -API in Beijing NSAQ stations, the mean bias of the hindcast decreases to  $-0.2$ , the normal mean error to 15.9%, and the correlation coefficient increases to 0.93. For  $PM_{10}$ -API in all stations in Beijing, the FAC2 increases from 56% in the forecast to 84% in the hindcast, while the NMSE decreases from 0.886 to 0.196. In the simulation of the  $PM_{10}$  hourly concentration, the correlation coefficient increases from 0.77 in the forecast to 0.88 in the hindcast, the FAC2 increases from 62% to 74%, and the NMSE decreases from 0.565 to 0.190. All of that illustrates the hindcast gives a much better model performance than the forecast in  $PM_{10}$  simulation in Beijing stations, not only the daily concentration but also hourly concentration.

The improvement methods we conducted in this study will be helpful to enhance the model performance in forecasting the air quality in Beijing and surrounding area. Especially the expanding model domain test indicated that the suitable domain setting is very important for the regional transport process, which is a key point in air quality forecasting not only in Beijing but also other similar regions. The modified emission inventory can also be used in the future forecasting and modeling works.

In the future, more model evaluation and improvement will continue in the air quality forecast in Beijing, to find other underestimated or overestimated cases in yearly forecasts and discover their causes, to improve the air quality forecast in those megacities, not only in Beijing.

## 5 Code availability

We use the original code CMAQ v4.4 as distributed by Community Modeling Analysis System(CMAS, <https://www.cmascenter.org/>). The model source code and the configuration, the library files and build scripts are all in the zipped file, which is accessible via  
5 FTP://159.226.119.102:/CMAQ2GMD.zip. The model runs on CentOS 5.5 Linux with PGI Fortran Compiler.

## Appendix A

### The air pollution index of particulate matter calculation

The model's SO<sub>2</sub>-API, NO<sub>2</sub>-API and PM<sub>10</sub>-API was calculated as followed, as defined  
10 by China EPB:

$$API = \frac{I_{\max} - I_{\min}}{C_{\max} - C_{\min}} \times (C - C_{\min}) + I_{\min},$$

where “C” is short for the concentration of the pollutant, and  $C_{\max}/C_{\min}$  were the classic concentration shown in the Table A1 near to “C”, and the  $I_{\max}/I_{\min}$  were their corresponding API values.

15 Take PM<sub>10</sub> API value for example: if the observation of PM<sub>10</sub> concentration is 0.12 mg m<sup>-3</sup>, then, the  $C = 0.12 \text{ mg m}^{-3}$ , and the  $C_{\max}$  and  $C_{\min}$  is 0.050 mg m<sup>-3</sup> and 0.150 mg m<sup>-3</sup>, respectively, the  $I_{\max}$  and  $I_{\min}$  was 50 and 100. Thus, the API of PM<sub>10</sub> concentration (0.12 mg m<sup>-3</sup>) was

$$API = \frac{100 - 50}{0.150 - 0.050} \times (0.12 - 0.050) + 50 = 85.$$



## Appendix B

### The statistical parameters

Mean bias:

$$MB = \frac{1}{n} \sum_{i=1}^n (\text{Sim}(i) - \text{Obs}(i)).$$

5 Normal mean error:

$$NME = \frac{1}{n} \sum_{i=1}^n |\text{Sim}(i) - \text{Obs}(i)| / \text{Obs}(i).$$

Correlation coefficient ( $R$ ):

$$R = \frac{\sum_{i=1}^n (\text{Sim}(i) - \overline{\text{Sim}})(\text{Obs}(i) - \overline{\text{Obs}})}{\sqrt{\sum_{i=1}^n (\text{Sim}(i) - \overline{\text{Sim}})^2 \sum_{i=1}^n (\text{Obs}(i) - \overline{\text{Obs}})^2}}.$$

The normalized mean square error (NMSE):

$$10 \text{ NMSE} = \frac{\overline{(\text{Obs} - \text{Sim})^2}}{\text{Obs} \times \text{Sim}}.$$

FAC2 (fraction of predictions within a factor of two of the observations) = fraction of data that satisfies:

$$0.5 \leq \frac{\text{Sim}(i)}{\text{Obs}(i)} \leq 2.0.$$

15 *Acknowledgements.* This study is funded by the National Natural Science Foundation of China (no. 41305121), the Fundamental Research Funds for the Central Universities and the Urban Meteorological Science Fund (no. UMRF201003).

## References

An, X., Zhu, T., Wang, Z., Li, C., and Wang, Y.: A modeling analysis of a heavy air pollution episode occurred in Beijing, *Atmos. Chem. Phys.*, 7, 3103–3114, doi:<http://dx.doi.org/10.5194/acp-7-3103-2007>, 2007.

5 Appel, K. W., Roselle, S. J., Gilliam, R. C., and Pleim, J. E.: Sensitivity of the Community Multi-scale Air Quality (CMAQ) model v4.7 results for the eastern United States to MM5 and WRF meteorological drivers, *Geosci. Model Dev.*, 3, 169–188, doi:<http://dx.doi.org/10.5194/gmd-3-169-2010>, 2010.

10 Binkowski, F. S. and Roselle, S. J.: Models-3 Community Multiscale Air Quality (CMAQ) model aerosol component 1. Model description, *J. Geophys. Res.-Atmos.*, 108, 4183, doi:<http://dx.doi.org/10.1029/2001JD001409>, 2003.

Briggs, G.: Discussions on chimney plumes in neutral and stable surroundings, *Atmos. Environ.*, 6, 507–510, 1972.

15 Briggs, G. A.: Plume rise and buoyancy effects, in: *Atmospheric Science and Power Production*, 327–366, 1984.

BTRC: Beijing Transport Annual Report 2006, Tech. rep., Beijing Transport Research Center, Beijing, China, 2007.

20 Byun, D. and Schere, K. L.: Review of the governing equations, computational algorithms, and other components of the Models-3 Community Multiscale Air Quality (CMAQ) modeling system, *Appl. Mech. Rev.*, 59, 51–77, 2006.

Byun, D. and Ching, J. K. S.: *Science Algorithms of the EPA Models-3 Community Multi-scale Air Quality (CMAQ) Modeling System*, Tech. Rep. EPA/600/R-99/030, US EPA National Exposure Research Laboratory, Research Triangle Park, NC, 1999.

25 Cao, G., Zhang, X., Gong, S., An, X., and Wang, Y.: Emission inventories of primary particles and pollutant gases for China, *Chinese Sci. Bull.*, 56, 781–788, 2011.

CCCPS: The Pollution Source Census Data Set (Statistic), *Collected Works about the First China Pollution Source Survey Data (V)*, Compilation Committee of China Pollution Source Census I, China Environment Science Press, Beijing, 228–245, 2011.

30 Chang, J. and Hanna, S.: Air quality model performance evaluation, *Meteorol. Atmos. Phys.*, 87, 167–196, 2004.

- Cruickshank, T. S.: CMAQ sensitivity to winter-time ground surface albedo, in: Proceedings of the 7th Annual Community Modeling and Analysis (CMAS) Conference: Model Evaluation and Analysis, Chapel Hill, NC, 2008.
- Demerjian, K. L., Schere, K. L., and Peterson, J. T.: Theoretical Estimates of Actinic (Spherically Integrated) Flux and Photolytic Rate Constants of Atmospheric Species in the Lower Troposphere, John Wiley & Sons, New York, NY, 369–459, 1980.
- Dobson, J. E., Bright, E. A., Coleman, P. R., Durfee, R. C., and Worley, B. A.: LandScan: a global population database for estimating populations at risk, *Photogramm. Eng. Rem. S.*, 66, 849–857, 2000.
- ENVIRON: User's Guide to the Comprehensive Air Quality Modeling System with Extensions (CAMx), Version 4.4, Tech. Rep. 10, p. 16, p. 29, 38–40, p. 30, p. 44, ENVIRON, 2002.
- Beijing EPB: State of the Environment Bulletin in the year 2010, available at: <http://www.bjepb.gov.cn/bjepb/341240/index.html> (last access: June 2011), 2011.
- Feng, Y., Wang, A., Wu, D., and Xu, X.: The influence of tropical cyclone Melor on PM<sub>10</sub> concentrations during an aerosol episode over the Pearl River Delta region of China: numerical modeling versus observational analysis, *Atmos. Environ.*, 41, 4349–4365, 2007.
- Gao, Y., He, J., and Wang, Z.: Simulation for impact of urbanization on meteorological conditions in Beijing area, *Journal of Meteorology and Environment*, 23, 58–64, 2007 (in Chinese).
- Gery, M. W., Whitten, G. Z., Killus, J. P., and Dodge, M. C.: A photochemical kinetics mechanism for urban and regional scale computer modeling, *J. Geophys. Res.-Atmos.*, 94, 12925–12956, 1989.
- Grell, G. A., Dudhia, J., and Stauffer, D. R.: A description of the Fifth-Generation Penn State/NCAR Mesoscale Model (MM5), Tech. Rep. NCAR/TN-398+STR, Natl. Cent. for Atmos. Res., Boulder, Colo., 1994.
- Hao, J., Wang, L., Shen, M., Li, L., and Hu, J.: Air quality impact of power plant emissions in Beijing, *Environ. Pollut.*, 147, 401–408, 2008.
- Houyoux, M. R. and Vukovich, J. M.: Updates to the Sparse Matrix Operator Kernel Emissions (SMOKE) modeling system and integration with Models-3, The Emission Inventory: Regional Strategies for the Future, Air Waste Management Association, Raleigh, N.C., 1461, 1999.
- Mobley, J. D., Beck, L. L., Sarwar, G., Reff, A., and Houyoux, M.: SPECIATE — EPA's Database of Speciated Emission Profiles, in: 6th Annual CMAS Conference,, U.S. Environmental Protection Agency, Chapel Hill, NC, 2007.

- Streets, D., Bond, T., Carmichael, G., Fernandes, S. D., Q. Fu, D. H., Klimont, Z., Nelson, S. M., Tsai, N. Y., Wang, M. Q., Woo, J. H., and Yarber, K. F.: An inventory of gaseous and primary aerosol emission in Asia in the year 2000, *J. Geophys. Res.-Atmos.*, 108, doi:<http://dx.doi.org/10.1029/2002JD003093>, 2003.
- 5 Streets, D., Zhang, Q., Wang, L., He, K., Hao, J., Wu, Y., Tang, Y., and Carmichael, G. R.: Revisiting China's CO emissions after the Transport and Chemical Evolution over the Pacific (TRACE-P) mission: synthesis of inventories, atmospheric modeling, and observations, *J. Geophys. Res.-Atmos.*, 111, doi:<http://dx.doi.org/10.1029/2006JD007118>, 2006.
- 10 Streets, D., Joshua, S. F., Carey, J., Hao, J., He, K., Tang, X., Zhang, Y., Wang, Z., Li, Z., Zhang, Q., Wang, L., Wang, B., and Yu, C.: Air quality during the 2008 Beijing Olympic Games, *Atmos. Environ.*, 41, 480–492, 2007.
- UNC: SMOKE v2.7 User's Manual, Tech. Rep. 98, The institute for the Environment – The University of North Carolina at Chapel Hill, 2010.
- 15 Wang, S., Zhao, M., Xing, J., Wu, Y., Zhou, Y., Lei, Y., He, K., Fu, L., and Hao, J.: Quantifying the air pollutants emission reduction during the 2008 Olympic Games in Beijing, *Environ. Sci. Technol.*, 44, 2490–2496, 2010.
- Wang, Z., Xie, F., Wang, X., An, J., and Zhu, J.: Development and application of nested air quality prediction modeling system, *Chinese J. Atmos. Sci.*, 30, 778–790, 2006 (in Chinese).
- 20 Wang, Z., Wu, Q., Gbaguidi, A., Yan, P., Zhang, W., Wang, W., and Tang, X.: Ensemble air quality multi-model forecast system for Beijing (EMS-Beijing): model description and preliminary application, *J Nanjing University Inform Sci Technol: Natural Science Edition*, 1, 19–26, 2009 (in Chinese).
- Wu, Q.: Air Quality Multi-models real-time forecast system in Beijing and its Air Quality Multi-models real-time forecast system in Beijing and its application, Ph.D. thesis, Institute of Atmospheric Physics, Chinese Academy of Sciences, Beijing, 2010a.
- 25 Wu, Q., Wang, Z., Xu, W., Huang, J., and Gbaguidi, A.: Multi-model simulation of PM<sub>10</sub> during the 2008 Beijing Olympic Games: effectiveness of emission restrictions, *Acta Scientiae Circumstantiae*, 30, 1739–1748, 2010a(in Chinese).
- 30 Wu, Q., Wang, Z., and Cui, Y.: Evaluating the solar radiation resources of China recent 20 years by meteorological model, *Journal of Applied Meteorological Science*, 21, 343–351, 2010b (in Chinese).

- Wu, Q., Wang, Z., Alex, G., Tang, X., and Zhou, W.: Numerical study of the effect of traffic restriction on air quality in Beijing, SOLA, 6A, 017–020, 2010c.
- Wu, Q., Wang, Z. F., Gbaguidi, A., Gao, C., Li, L. N., and Wang, W.: A numerical study of contributions to air pollution in Beijing during CAREBeijing-2006, *Atmos. Chem. Phys.*, 11, 5997–6011, doi:<http://dx.doi.org/10.5194/acp-11-5997-2011>, 2011.
- 5 Wu, Q., Wang, Z., Chen, H., Zhou, W., and Wenig, M.: An evaluation of air quality modeling over the Pearl River Delta during November 2006, *Meteorol. Atmos. Phys.*, 116, 113–132, doi:<http://dx.doi.org/10.1007/s00703-011-0179-z>, 2012.
- Zhang, M., Uno, I., Zhang, R., Han, Z., Wang, Z., and Pu, Y.: Evaluation of the Models-3 Community Multi-scale Air Quality (CMAQ) modeling system with observations obtained during the TRACE-P experiment: comparison of ozone and its related species, *Atmos. Environ.*, 40, 4874–4882, 2006.
- Zhang, Q., Streets, D. G., Carmichael, G. R., He, K. B., Huo, H., Kannari, A., Klimont, Z., Park, I. S., Reddy, S., Fu, J. S., Chen, D., Duan, L., Lei, Y., Wang, L. T., and Yao, Z. L.: Asian emissions in 2006 for the NASA INTEX-B mission, *Atmos. Chem. Phys.*, 9, 5131–5153, doi:<http://dx.doi.org/10.5194/acp-9-5131-2009>, 2009.
- 15 Zhao, B., Wang, P., Ma, J. Z., Zhu, S., Pozzer, A., and Li, W.: A high-resolution emission inventory of primary pollutants for the Huabei region, China, *Atmos. Chem. Phys.*, 12, 481–501, doi:<http://dx.doi.org/10.5194/acp-12-481-2012>, 2012.
- 20 Zhao, X. J., Zhao, P. S., Xu, J., Meng, W., Pu, W. W., Dong, F., He, D., and Shi, Q. F.: Analysis of a winter regional haze event and its formation mechanism in the North China Plain, *Atmos. Chem. Phys.*, 13, 5685–5696, doi:<http://dx.doi.org/10.5194/acp-13-5685-2013>, 2013.

**Table 1.** Emission of major anthropogenic species (Unit:  $10^3 \text{ tyr}^{-1}$ ).

Species	Region	CO	NO <sub>x</sub>	VOCs	NH <sub>3</sub>	SO <sub>2</sub>	PM <sub>10</sub>	PM <sub>2.5</sub>
In forecast system	Beijing	1793.8	200.0	244.2	121.8	78.8	162.1	59.1
	Tianjin	1609.9	275.3	270.7	47.2	353.5	194.1	132.7
	Hebei	6504.3	983.1	839.6	837.0	1966.7	997.6	712.4
An et al. (2007)	Beijing	1021.8	227.3	285.6	69.1	211.3	106.9	53.4
	Tianjin	737.0	178.9	270.0	50.0	375.9	93.5	38.0
	Hebei	6806.0	686.0	855.0	846.5	1353.7	535.1	264.1
Streets et al. (2007)*	Beijing	2340.0	212.4	339.6	150.0	318.0	66.0	27.2
	Tianjin	1704.0	272.4	272.4	118.9	409.2	80.5	31.6
	Hebei	6540.0	704.4	864.0	1812.0	1272.0	463.2	199.2
Zhang et al. (2009)	Beijing	2591.0	327.0	497.0	–	248.0	123.0	90.0
	Tianjin	1860.0	365.0	381.0	–	336.0	161.0	109.0
	Hebei	15505.0	1308.0	1521.0	–	2281.0	1371.0	981.0
Cao et al. (2011)	Beijing	1998.0	437.0	744.0	117.0	172.0	–	162.0
	Tianjin	1625.0	337.0	467.0	102.0	263.0	–	151.0
	Hebei	12669.0	1634.0	2327.0	994.0	2318.0	–	1172.0
Zhao et al. (2012)	Beijing	2580.0	309.0	346.0	87.0	187.0	168.0	90.0
	Tianjin	1326.0	177.0	224.0	74.0	259.0	186.0	100.0
	Hebei	12202.0	1092.0	757.0	1031.0	1622.0	2291.0	1214.0

\* Streets et al. (2007): for July 2001, convert unit  $\text{Gg mol}^{-1}$  to  $\text{Ggyr}^{-1}$ .

**Table 2.** Statistical measures of the modeled NSAQ station-averaged PM<sub>10</sub>-API in Beijing.

	Obs	Forecast	FEmis+ omain(CMAQ)	NewD	NewEmis+FD omain(CMAQ)	New(CMAQ)
peak	183	96		140	105	180
MB	-	-24.7		-15.4	-24.3	-0.2
NMSE	-	0.251		0.082	0.212	0.042
R	-	0.895		0.943	0.888	0.931

**Table 3.** Statistical measures of the modeled daily PM<sub>10</sub>-API in all stations in Beijing.

	Obs	Forecast	FEmis+ omain(CMAQ)	NewD omain(CMAQ)	NewEmis+FD omain(CMAQ)	New(CMAQ)
peak	327	139		187	138	220
MB	-	-43.2		-30.4	-36.0	-15.7
NMSE	-	0.886		0.386	0.558	0.196
FAC2	-	56%		70%	68%	84%
R	-	0.54		0.78	0.72	0.82



**Table A1.** The API values and corresponding pollutant concentration (daily, Unit:  $\text{mg m}^{-3}$ ).

API	SO <sub>2</sub>	NO <sub>2</sub>	PM <sub>10</sub>
50	0.05	0.08	0.05
100	0.15	0.12	0.15
200	0.80	0.28	0.35
300	1.60	0.565	0.42
400	2.10	0.75	0.50
500	2.62	0.94	0.60

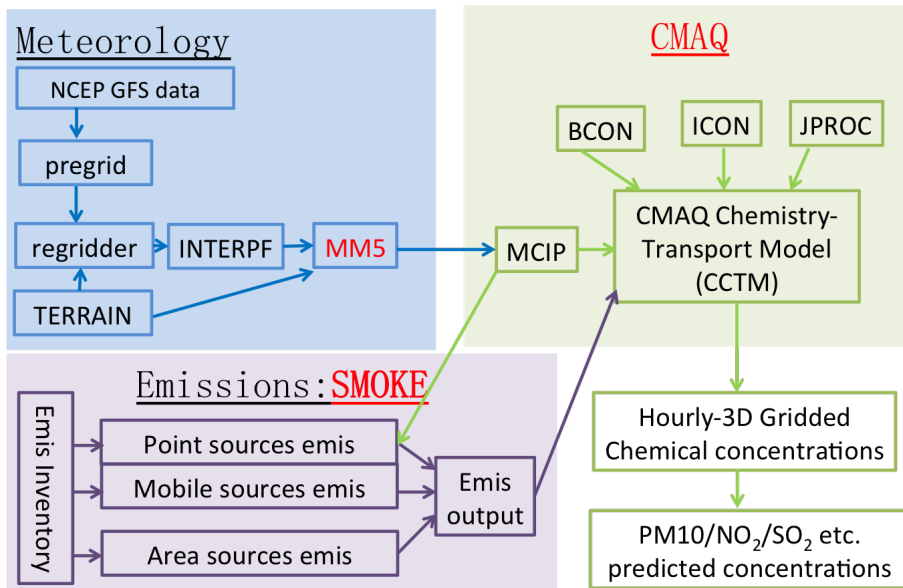


**Fig. 1.** The framework of the MM5-SMOKE-CMAQ forecast system in Beijing.

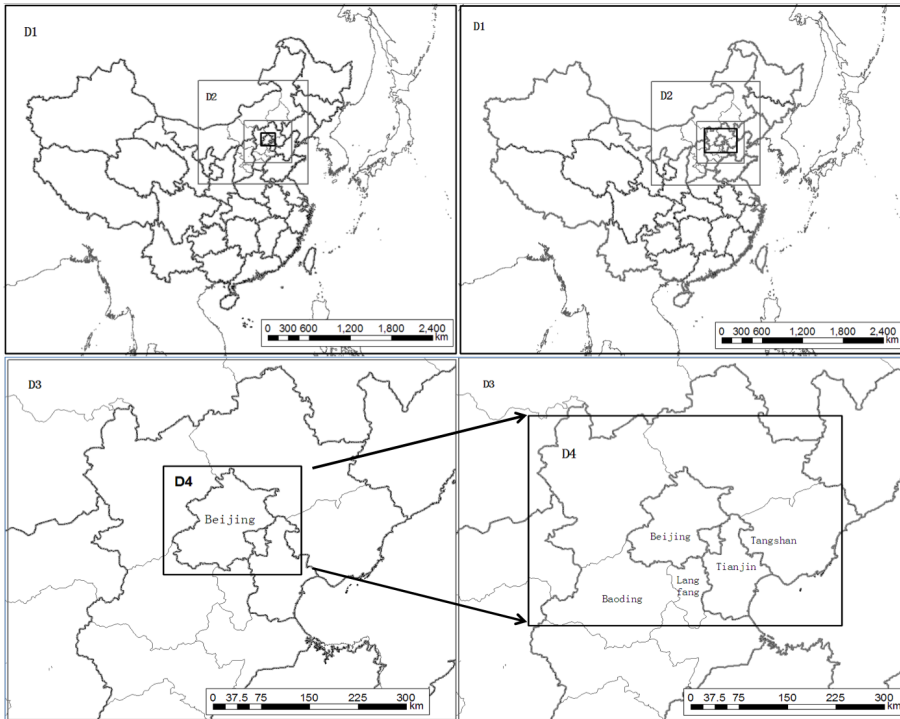


**Fig. 2.** The four nest domain used in the forecast system and the “new” enhanced domain in the hindcast. Left, the forecast system: D1 covers East Asia with 81 km horizontal resolution and  $83 \times 65$  grids. D2 includes North China as shown in the upper. D3 consists Beijing, Tianjin and most area of Hebei province, but D4 only cover Beijing Municipality with  $73 \times 64$  grids of 3 km resolution as shown in the lower left. On the right, the domain for the “new” simulation (hindcast) in this study, we enlarge the inner D4 domain with  $160 \times 124$  grids of 3 km resolution, and covers Beijing and its surrounding municipal cities, including Tianjin, Baoding, Langfang and Tangshan.

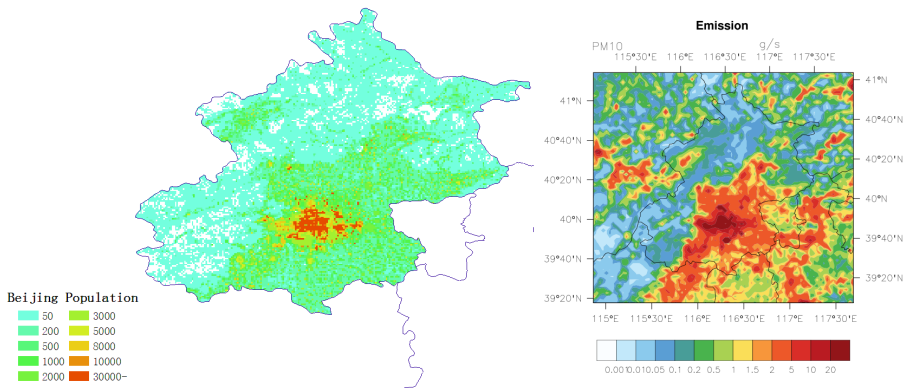


**Fig. 3.** The SMOKE-area emissions have been spatially allocated based on the related spatial factor, such as its population data provided from Land Scan 2005 Global Population Database (Dobson et al., 2000). The left is the spatial distribution of the population in Beijing Municipality in the Land Scan 2005; the right is the spatial distribution of the PM<sub>10</sub> emissions in the inner domain in the forecast system.

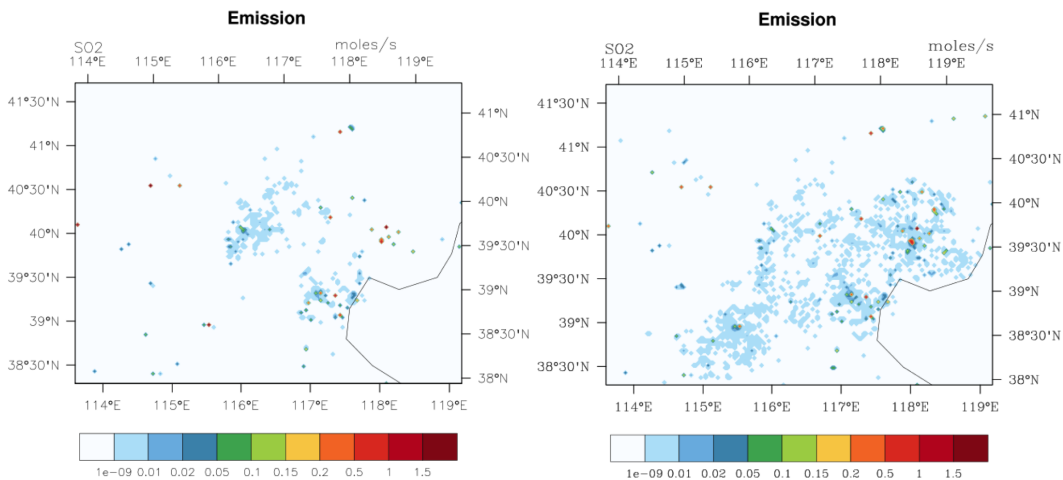


**Fig. 4.** The point source emissions in the “new” D4 domain. Left is the point source emissions in the forecast system, while the right is in the “new” simulation; more point source emissions in Tangshan, Baoding and Langfang have been added.

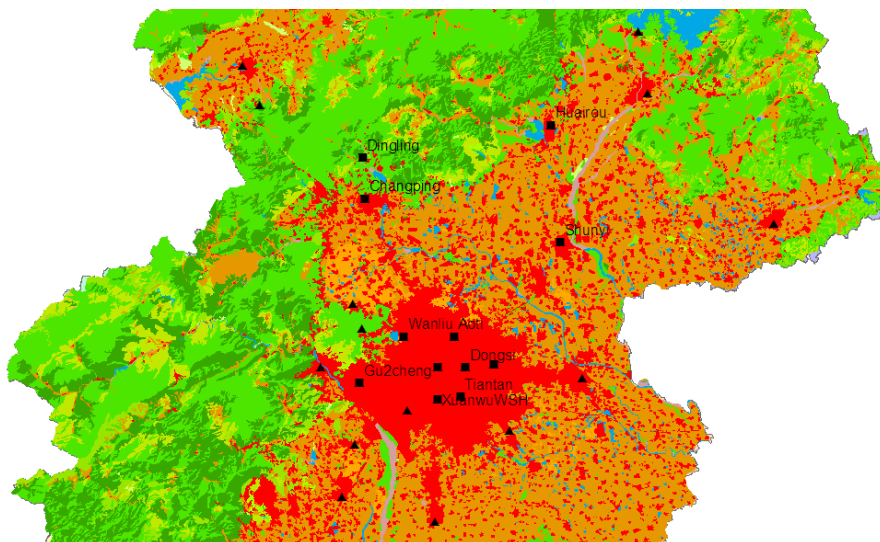


**Fig. 5.** The stations map of Beijing MEMC air quality monitoring network. Black shows the location of each observation station, squares are the National Standard Air Quality Observation Stations (NSAQ Stations), and triangles are the other air quality observation stations in the monitoring network. The shaded indicates land use, red shaded indicates urban area, dark green indicates forest, light green indicates grass, orange indicates crop, blue indicates water.

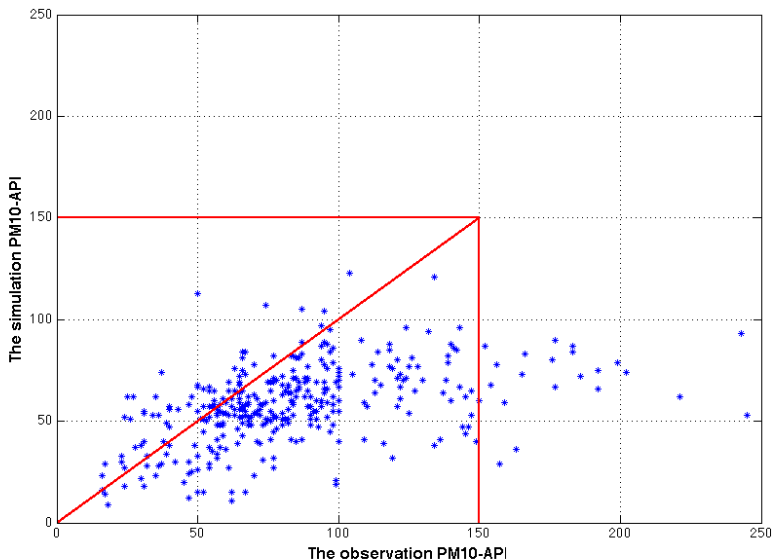


**Fig. 6.** The observed-simulated scatter diagram of the averaged  $PM_{10}$ -API in the Beijing NSAQ stations in 2010. The averaged NSAQ stations include Aoti, Dongsi, Wanliu, Chegongzhuang, Gu2cheng, Tiantan, XuanwuWSH, Nongzhanguan, Changping, Shunyi and Huairou stations.

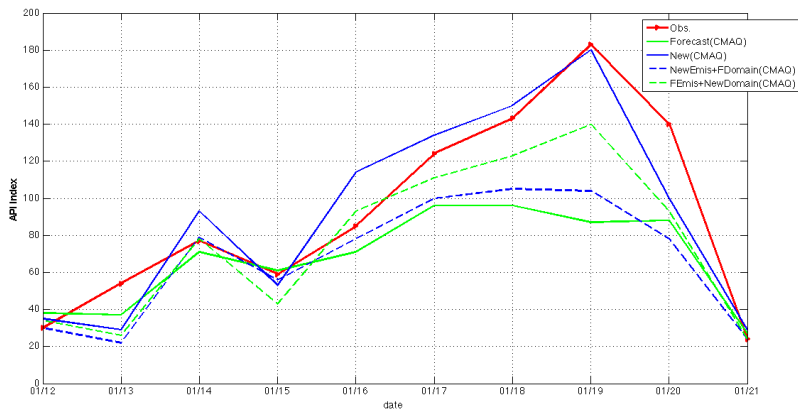


**Fig. 7.** Comparison of measured and modeled daily averaged  $PM_{10}$ -API in the NSAQ stations in Beijing urban area. After the improvement in model domain and emission, the “New(CMAQ)” results reach to the peak of the observation, which the forecast underestimated.



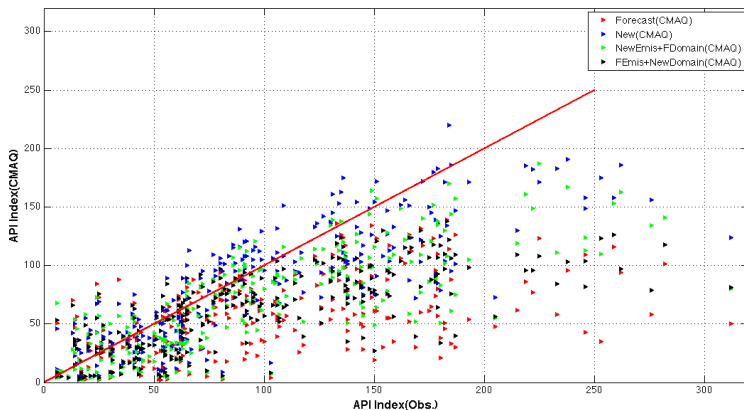


**Fig. 8.** The scatter diagram of the observed and simulated  $PM_{10}$ -API in all stations in Beijing. The red is the original forecast results, and the blue triangle is the final model results, which is driven by the updated emissions in the expanded model domain, marker as “New(CMAQ)”.

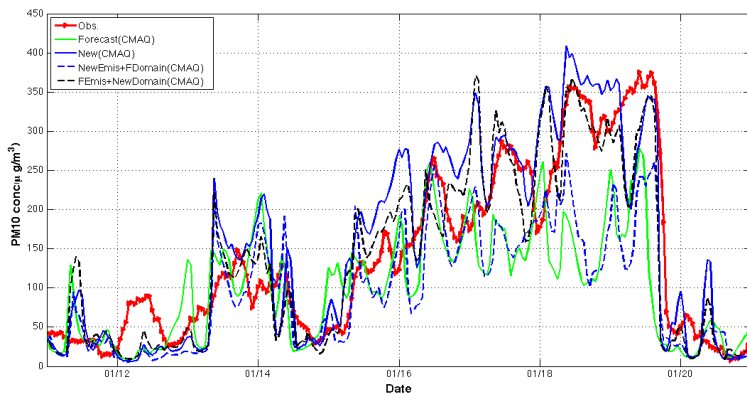


**Fig. 9.** The time series of the  $PM_{10}$  hourly concentration during the air pollution episode in January 2010. The red solid line is the observation, which is the averaged  $PM_{10}$  hourly concentration observed in the ten NSAQ stations in Beijing MEMC monitoring network. The “New(CMAQ)” shows a much better model performance about the hourly concentration during the air pollution episode than the forecast due to the improvement of model domain and emissions.